AGU PUBLICATIONS

JGR

Journal of Geophysical Research: Atmospheres

RESEARCH ARTICLE

10.1002/2016JD025472

Key Points:
- Significant positive trends of OMI AAOD in the U.S. over 2005–2015 are identified
- The positive trends of AAOD are found not to be dominated with absorbing carbonaceous aerosols from U.S. anthropogenic local emissions
- Positive trends of AAOD are partially associated with increasing concentrations of coarse dust

Correspondence to:
L. Zhang,
li.zhang@colorado.edu

Citation:
Zhang, L., D. K. Henze, G. A. Grell, O. Torres, H. Jethva, and L. N. Lamsal (2017), What factors control the trend of increasing AAOD over the United States in the last decade?, *J. Geophys. Res. Atmos.*, *122*, 1797–1810, doi:10.1002/2016JD025472.

Received 7 JUN 2016
Accepted 25 JAN 2017
Accepted article online 27 JAN 2017
Published online 7 FEB 2017

What factors control the trend of increasing AAOD over the United States in the last decade?

Li Zhang[1,2,3], Daven K. Henze[2], Georg A. Grell[3], Omar Torres[4], Hiren Jethva[5], and Lok N. Lamsal[4,5]

[1]Cooperative Institute for Research in Environmental Sciences, University of Colorado Boulder, Boulder, Colorado, USA, [2]Department of Mechanical Engineering, University of Colorado Boulder, Boulder, Colorado, USA, [3]Global Systems Division, Earth System Research Laboratory, NOAA, Boulder, Colorado, USA, [4]NASA Goddard Space Flight Center, Greenbelt, Maryland, USA, [5]GESTAR/University Space Research Association, NASA Goddard Space Flight Center, Greenbelt, Maryland, USA

Abstract We examine the spatial and temporal trends of absorbing aerosol optical depth (AAOD) in the last decade over the United States (U.S.) observed by the Ozone Monitoring Instrument (OMI). Monthly average OMI AAOD has increased over broad areas of the central U.S. from 2005 to 2015, by up to a factor of 4 in some grid cells (~60 km resolution). The AAOD increases in all seasons, although the percentage increases are larger in summer (June-July-August) than in winter (December-January-February) by a factor of 3. Despite enhancements in AAOD, OMI AOD exhibits insignificant trend over most of the U.S. except parts of the central and western U.S., the latter which may partly be due to decreases in precipitation. Trends in AAOD contrast with declining trends in surface concentrations of black carbon (BC) aerosol. Interannual variability of local biomass burning emissions of BC may contribute to the positive trend in AAOD over the western U.S. Changes in both dust aerosol measured at the surface (in terms of concentration and size) and dust AAOD indicate distinct enhancements, especially over the central U.S. by 50–100%, which appears to be one of the major factors that impacts positive trends in AAOD.

1. Introduction

The importance of aerosol forcing on climate has been widely recognized [*Myhre et al.*, 2013]. Aerosol effects on climate depend upon several physical characteristics, such as size, composition, and optical properties (especially absorption) [*Myhre*, 2009]. Carbonaceous particles (black carbon (BC) and brown carbon) and mineral dust are two major absorbing aerosols present in the atmosphere. Normally, BC aerosol absorbs across much of the solar spectrum, while organic carbon (OC) strongly absorbs in the UV and visible wavelengths but have weak absorption in the near infrared [*Lewis et al.*, 2008; *Lack and Cappa*, 2010; *Logan et al.*, 2013]. Mineral dust has similar absorptive properties to OC but primarily absorbs in the shortwave spectrum [*Bergstrom et al.*, 2007; *Russell et al.*, 2010]. Remote sensing of absorbing aerosol from satellite-based sensors provides a means of detecting and monitoring global trends in aerosol concentrations [*Jethva et al.*, 2014]. The absorbing aerosol optical depth (AAOD), the nonscattering part of aerosol optical depth (AOD), is a measurement of absorbing aerosol particles, light-absorbing OC, and dust. Trends in observed AAOD have important implications for understanding the climate forcing due to absorbing aerosols, evaluating the effectiveness of past control strategies, and the design of future policy.

Several domestic and international factors may potentially impact trends in AAOD in the U.S. Surface-level concentrations of BC in the U.S. have been declining [*Murphy et al.*, 2011; *Bahadur et al.*, 2011]. Observations at national parks and other remote sites show that average elemental carbon (EC) concentrations in the U.S. decreased by over 25% between 1990 and 2004 due to the emission controls in diesel vehicles and wood stoves [*Murphy et al.*, 2011]. Regional declines in BC aerosol concentrations may be even stronger, as they have declined by 50% in California between 1989 and 2008 following a parallel trend in the reduction of fossil fuel BC emissions [*Bahadur et al.*, 2011]. In contrast, oil and gas development in the Bakken shale extending over northwestern North Dakota and southeast Saskatchewan have lead to increased concentrations of BC [*Schwarz et al.*, 2015].

For dust, AOD over the mid-Atlantic has decreased by ~10% per decade from 1982 to 2008 [*Ridley et al.*, 2014]. *Shao et al.* [2013] found that global mean (excluding North America and Europe) near-surface dust concentrations decreased by 1.2% yr^{-1} over the period of 1984–2012. This decrease is mainly due to

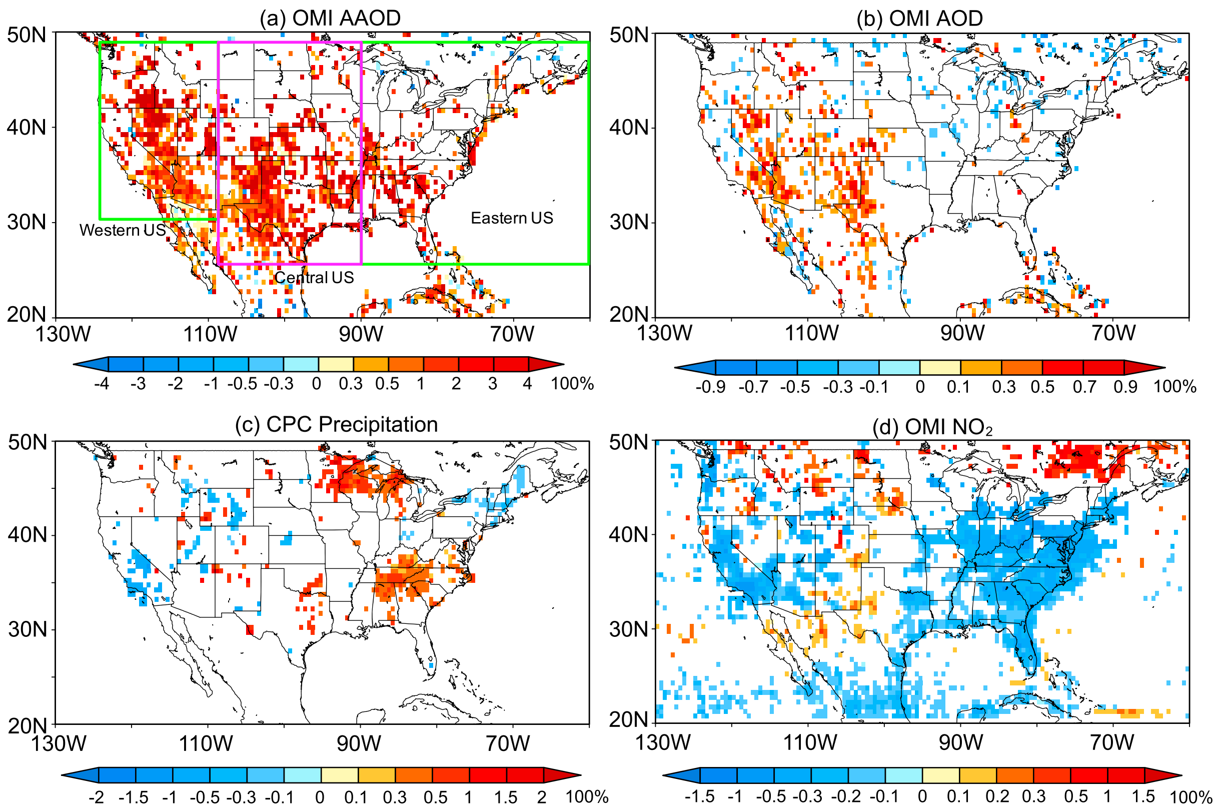

Figure 1. The trends of percentage changes (unit: 100%) for (a) OMI AAOD, (b) OMI AOD, (c) GPCC precipitation, and (d) OMI column NO_2 for 2005–2015. Only areas with 90% confidence are shown.

climate change that reduced natural dust activity in North Africa, accompanied by reduced activity in Northeast Asia, South America, and South Africa. The magnitude of dust emissions is very sensitive to regional climate (e.g., surface wind speed and soil characteristics) since dust concentrations decrease with increasing precipitation owing to wet deposition [*Dawson et al.*, 2007; *Mu and Liao*, 2014].

Long-range transport may also contribute to trends in AAOD in the U.S. Southeast Asia is a major anthropogenic BC source region, with an increase in BC emissions of 21% over China and 41% over India from 1996 to 2010 associated with rapid economic and industrial development [*Lu et al.*, 2011]. The rapid economic growth and vast expansion of producing goods for export in Asia over the past decade have been detected in significant increasing aerosol optical depth (AOD) trends over the largest cities in the India and North China during 2002–2010 [*Alpert et al.*, 2012]. The impacts of these emissions also extend to downwind regions, e.g., the U.S. [*Lin et al.*, 2012]. *Hadley et al.* [2007] pointed out that over 75% of the BC transport to the northern Pacific Ocean originates in Asia during spring (March-April-May (MAM)) in 2004, and this transport amounts to approximately 77% of the published estimates of North American BC emissions. Also, dust from the Taklimakan and Gobi deserts in Asia can be transported over the North Pacific Ocean and reach North America [*Huang et al.*, 2008; *Eguchi et al.*, 2009]. The annual imported mass of dust aerosol from transpacific transport over North America is comparable in magnitude to all domestic aerosol sources, which makes a substantial contribution to AOD in North America away from strong anthropogenic sources [*Yu et al.*, 2012].

In this paper we analyze data from the Ozone Monitoring Instrument (OMI) to investigate the AAOD trends in the U.S. between 2005 and 2015. The results show significant positive trends in AAOD of 100–400% over large regions of the U.S. (Figure 1a). This raises a question as to what is the major factor controlling the positive trend of AAOD over U.S. Addressing this question entails evaluating the impacts of increasing anthropogenic BC emissions in Asia, declining surface BC concentrations in U.S., and changes of climate that result in changes of dust emission, precipitation, or long-range aerosol transport. Section 2 describes the model and observation data used in this study. We then investigate the AAOD trends for 2005–2015 in section 3. Section 4 evaluates the AAOD trend, and we end with discussion and conclusions in section 5.

2. Model and Observations

2.1. Goddard Earth Observing System-Chemistry Model

Goddard Earth Observing System-Chemistry (GEOS-Chem) is a global three-dimensional chemical transport model driven by assimilated meteorological observations from the Goddard Earth Observing System (GEOS) [*Bey et al*., 2001]. We use GEOS-Chem version 9-01-01 driven by GEOS 5 meteorological fields, 2° (latitude) × 2.5° (longitude) horizontal resolution, and 47 vertical layers between the surface and 0.01 hPa. The original carbonaceous aerosol simulation in GEOS-Chem was developed by *Park et al*. [2003]. It assumes that 80% of BC and 50% of OC emitted from primary sources are hydrophobic and that hydrophobic aerosols become hydrophilic with an *e*-folding time of 1.15 days [*Park et al*., 2003; *Chin et al*., 2002; *Cooke et al*., 1999]. Dust in GEOS-Chem is distributed across four size bins (radii 0.1–1.0, 1.0–1.8, 1.8–3.0, and 3.0–6.0 μm) following *Ginoux et al*. [2004]. The wet deposition scheme [*Liu et al*., 2001] includes scavenging in convective updrafts as well as in-cloud and below-cloud scavenging from convective and large-scale precipitation. Dry deposition is based on the resistance-in-series scheme of *Wesely* [1989] as implemented by *Wang et al*. [1998].

Global anthropogenic emissions for carbonaceous aerosols (BC and OC) in GEOS-Chem are originally from *Bond et al*. [2004, 2007], which contain both biofuel and fossil fuel emissions. For biomass burning emissions of BC, the fourth generation of the Global Fire Emissions Database (GFED) burned area data set GFED4, which provides global monthly burned area at 0.25° spatial resolution from 2005 to 2015, has been used [*Giglio et al*., 2013]. The standard dust emission scheme in GEOS-Chem is the dust entrainment and deposition mobilization scheme of *Zender et al*. [2003], combined with the source function used in the Global Ozone Chemistry Aerosol Radiation and Transport model [*Ginoux et al*., 2001; *Chin et al*., 2002] as described by *Fairlie et al*. [2007]. A new emitted dust particle size distribution based upon scale-invariant fragmentation theory [*Kok*, 2011b] with constraints from in situ measurements [*Zhao et al*., 2010] is implemented in GEOS-Chem to improve the dust simulation [*Zhang et al*., 2013].

Aerosol optical depth at 400 nm is calculated online assuming lognormal size distributions of externally mixed aerosols and is a function of the local relative humidity to account for hygroscopic growth [*Martin et al*., 2003]. The AAOD of each aerosol species is calculated as AAOD = AOD*(1-SSA), where SSA is the single scattering albedo [*Ma et al*., 2012; *Zhang et al*., 2015].

2.2. OMI Measurements

OMI, aboard the Aura satellite, is a nadir-viewing, wide-swath hyper-spectral imaging spectrometer that provides measurements with daily global coverage and high spectral resolutions and spatial resolution of $13 \times 24\ km^2$ at nadir [*Levelt et al*., 2006]. Version 1.4.2 level 2 monthly data are used in this study. OMI takes advantage of the sensitivity of radiances measured at the atmosphere in the near-UV region to the varying load and type of aerosols to derive extinction AOD, single scattering albedo (SSA), and AAOD using the near-UV (OMAERUV) algorithm [*Torres et al*., 2007] for observations at 354 nm, 388 nm, and 500 nm. Aerosol retrievals with quality flag 0 are considered to be the best in accuracy as this category of flag scheme largely avoids cloud contaminated pixels by choosing the appropriate reflectivity and UV-aerosol index (AI) thresholds [*Jethva et al*., 2014]. Given that the uncertainty of the retrieved SSA at low AOD values is larger, the operational algorithm assumed a SSA of unity (1.0) for pixels having lower values of UV-AI, which thereby exclude the very small AOD values (associated with small and negative aerosol index values) in calculating the monthly average. OMAERUV retrievals of AOD and SSA have been evaluated by comparison to independent ground-based observations provided by the world-wide Aerosol Robotic Network (AERONET). OMAERUV AOD retrievals at 380 nm were compared to AERONET observations [*Ahn et al*., 2014]. The AERONET-OMAERUV analysis yields a correlation coefficient of 0.81, *y* intercept of 0.1, and slope of 0.79. The OMAERUV SSA product has also been evaluated by using AERONET retrievals. *Jethva et al*. [2014] compared OMAERUV and AERONET SSA retrievals by using all available AERONET data at 269 sites for the 2005–2013 period. After accounting for the wavelength difference (AERONET 440 nm versus OMAERUV 388 nm), it was shown that 50% of the matched OMAERUV-AERONET SSA pairs agree with AERONET values within 0.03, whereas 75% of the matched pairs agree within 0.05 for all aerosol types. Good agreement was also found between OMAERUV (version 1.4.2, operational) and AERONET for sites located in North America; the root-mean-square difference was about 0.04, while percentage matchups constrained within ±0.03 and ±0.05 were 57% and 82%, respectively.

The OMAERUV retrieval algorithm is particularly sensitive to carbonaceous and mineral aerosols. It assumes that the column aerosol load can be represented by one of three types of aerosols and uses a set of aerosol models to account for the presence of these aerosols: carbonaceous aerosol from biomass burning, desert dust, and weakly absorbing sulfate-based aerosols. The selection of an aerosol type relies on the OMI absorbing aerosol index ($UVAI_0$) and the Atmospheric Infrared Sounder total column carbon monoxide measurements as described in *Torres et al*. [2013]. Each aerosol type is represented by seven aerosol models of varying single scattering albedo, for a total of 21 models. The 21 aerosol models used by OMAERUV are based on long-term statistics of ground-based observations by AERONET.

Since early 2008, OMI's spatial coverage began to decrease at the onset of the so-called row anomaly, a physical obstruction initially affecting two of OMI's 60 viewing positions (or rows) in June 2007, currently extending to over 50% of the sensor's 60 rows. Although the exact nature of the problem is not known, it is suspected that the observed obstruction has developed as a result of the loosening of fabric material covering the interior walls of the sensor. The OMI row anomaly is not static as it slowly evolves over time at both long and short time scales affecting the quality of both level 1B spectral radiances and Level 2 products. As a consequence of the row anomaly, the global coverage attainable daily during the first 4 years of operation is no longer possible. Global coverage is currently achieved in about 2 days.

OMI monitors NO_2 column density by measuring spectral variation in backscattered solar radiation in the broad visible spectral window between 405 nm and 465 nm. OMI measurements are made in the early afternoon (i.e., local time of 13:00–14:45) with a spatial resolution of $13 \times 24\ km^2$ at nadir and with nearly daily global coverage. In this study, we use the improved OMI NO_2 retrieval that uses new a priori NO_2 profiles simulated by the NASA Global Modeling Initiative chemical transport model [*Lamsal et al*., 2015].

2.3. In Situ Measurements

Long-term measurements of fine aerosols (aerodynamic diameter at $<2.5\ \mu m$) for EC, OC, dust, and coarse PM (particulate matter between 2.5 and 10 μm in aerodynamic diameter) are available in the U.S. since 1987 from the Interagency Monitoring of Protected Visual Environments (IMPROVE) network for the protection of visibility in Class I remote areas (data available at http://vista.cira.colostate.edu/improve/ [*Malm et al*., 1994]). Surface soil dust concentrations are calculated as the sum of the soil-derived elements (Al, Si, K, Ca, Ti, and Fe) and their normal oxides [*Malm et al*., 1994]. Fine dust mass is estimated by using the formula of *Malm et al*. [1994].

3. AAOD Trends for 2005–2015

Figure 1a illustrates the spatial trends of percentage changes of OMI AAOD for 2005–2015. Only areas that exhibit a trend at the 90% confidence level are shown. The significance of the regression coefficients is tested by using the nonparametric Mann-Kendall tau test [*Sneyers*, 1990]. A significant positive trend is shown over broad areas of the U.S., with the maximum increase in an individual grid box being more than a factor of 4. The largest positive trends are mainly over the central U.S. and western U.S., such as Texas, western Oklahoma, Kansas, Nebraska, New Mexico, Colorado, South Dakota, North Dakota (by 200% to 400%). The AAOD trends in areas of the western U.S., such as California, Oregon, Washington, Nevada, and southwestern Arizona, also show enhancements by 50%–300% from 2005 to 2015. Areas of decreasing trends in the U.S. are evident, yet sparse. They do not occur with continuous spatial coverage and are mostly present in individual grid boxes in the northeastern U.S. The seasonality of the AAOD trends has also been investigated (see Figure 2). Positive trends are evident throughout all seasons to different extents. The largest increases are mainly over the western U.S. in summer (June-July-August (JJA)). The largest spatial extents of positive trends are in the summer (JJA) over most of the western and southern U.S., especially Nevada, eastern Oregon, Southern California, Arizona, Texas, Oklahoma, Kansas, and some states over southeastern U.S. More individual grid boxes indicate positive trends in the fall (September-October-November (SON)) than other seasons over the eastern U.S.

In addition to evaluating observed trends in OMI AAOD, we also used the GEOS-Chem model to simulate AAOD for 2005–2013. The model simulation using fixed anthropogenic emissions (without interannual variability) does not reproduce the observed positive trends of AAOD over the U.S., but it only simulates very slight positive trends over the central and northeastern areas, owing to increasing dust AAOD. However, these

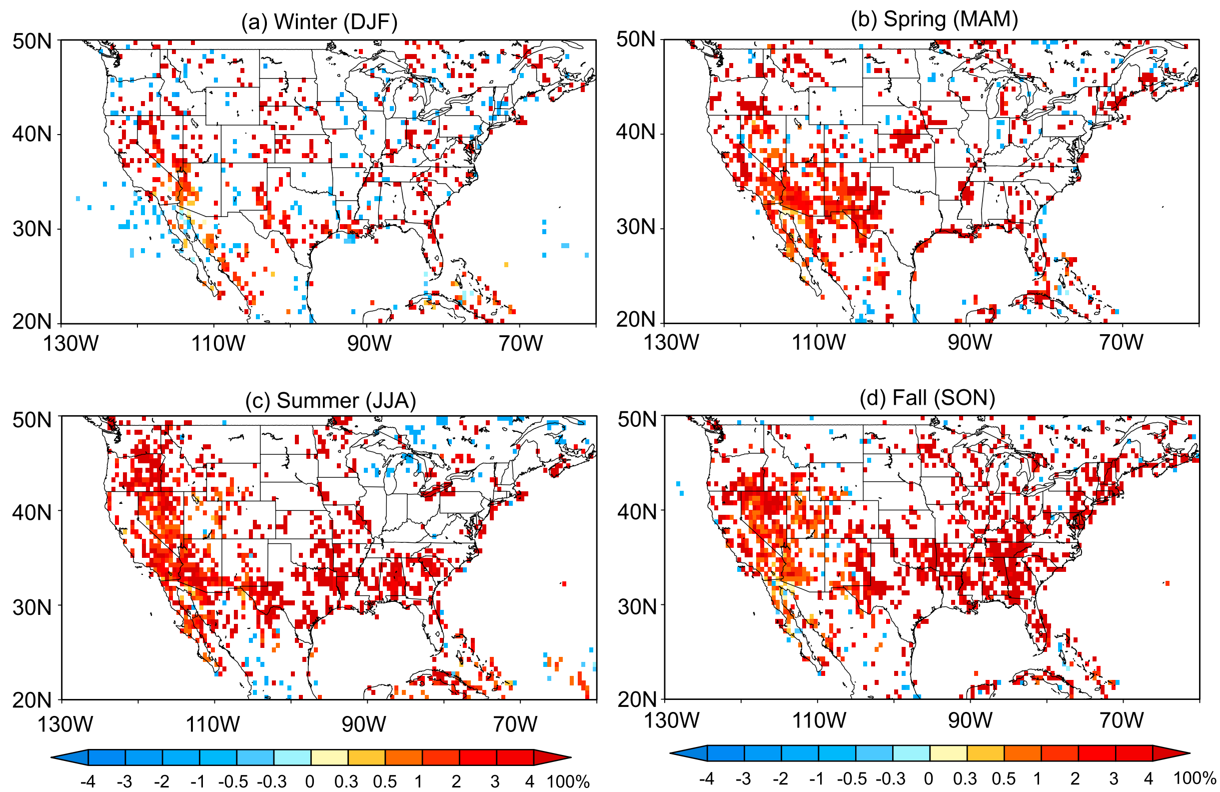

Figure 2. The trends of percentage changes (unit: 100%) for OMI AAOD for the seasons of (a) December-January-February, winter; (b) MAM, spring; (c) JJA, summer; and (d) SON, fall for 2005–2015. Only areas with 90% confidence are shown.

trends were not statistically significant. Modeled AAOD showed decreasing trends in total AAOD, BC AAOD, and OC AAOD. Also, there are not significant trends for biomass burning emissions throughout the U.S. in all seasons.

4. Evaluation of AAOD Trends

The trends identified in the data described in the previous section were somewhat surprising, given what is known about trends in surface-level BC concentrations. Thus, here we explore several factors that may be driving these AAOD trends, such as the changes of AOD, precipitation, NO_2, dust AAOD, surface absorbing aerosols, and biomass burning emissions.

One key to understanding the factors driving these observed trends in AAOD is the trends in AOD itself. Although AAOD is associated with AOD and SSA, the trend of OMI AOD is quite different to that of AAOD. Figure 1b shows that AOD trends are not as significant as those of AAOD and even shows slight decreasing trend over some areas of the U.S., except some areas over central and western U.S. These trends are not consistent with those of AAOD, with exceptions in the latter locations discussed further below. The largest decreasing AOD trends of −90% and −50% over the last decade are located over the northeastern and part of northwestern U.S., respectively. The reductions of AOD are also more evident in observations from satellites other then OMI, such as Multiangle Imaging Spectroradiometer (MISR) and Moderate Resolution Imaging Spectroradiometer (MODIS). Figure 3 shows the AOD trends of MISR, MODIS_TERRA, and MODIS_AQUA for 2005–2015. Although the trends of MISR AOD show increases over larger spatial areas of the western U.S. compared to OMI and MODIS, the general pattern is still similar. While the patterns of AOD trends in MODIS observations show a positive trend over the northern U.S., they are otherwise consistent with those of OMI, with enhancements over the central U.S. and reductions over other areas.

In contrast to the negative trend observed over most regions, AOD actually increases in Nevada, Arizona, New Mexico, Texas, Utah, and Colorado. Recall that these are the same locations where AAOD is also increasing. Figures 4a and 4b compare the trends of AAOD and AOD for 2005–2015 over the U.S. (20–50°N, 60–130°W)

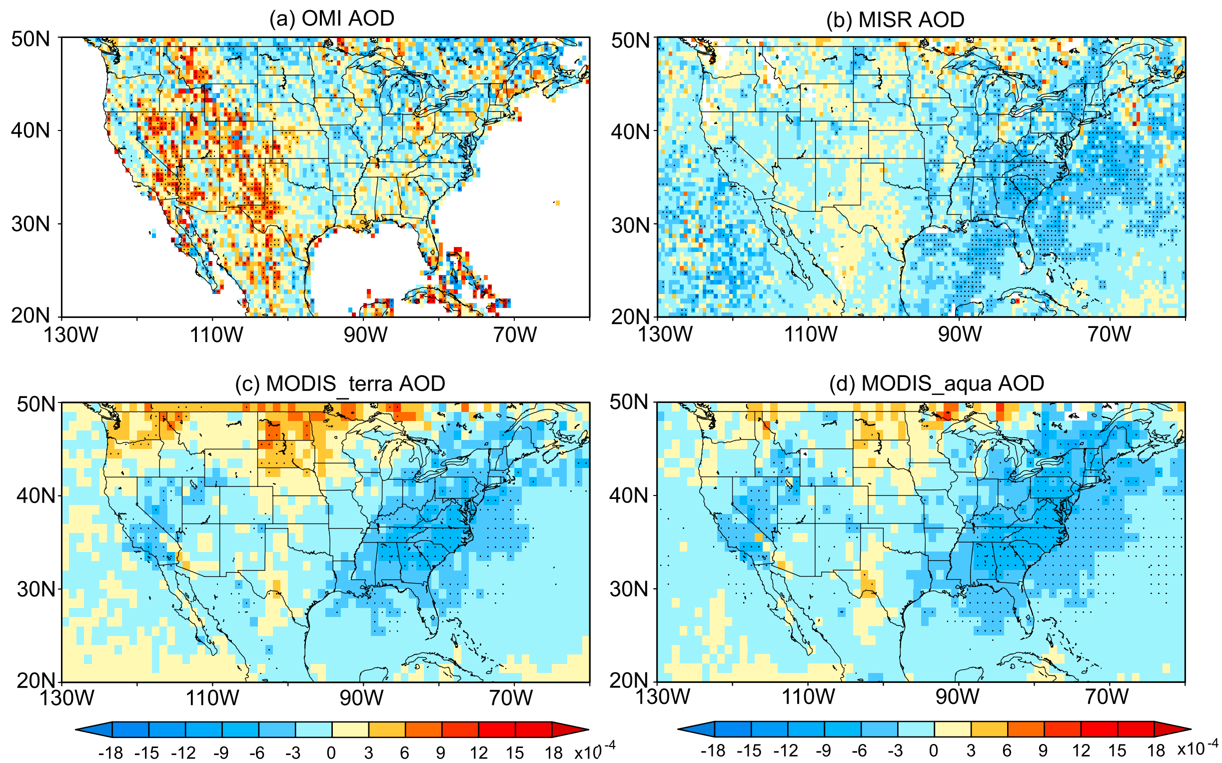

Figure 3. The monthly regression coefficients (10^{-4}) of (a) OMI AOD, (b) MISR AOD, (c) MODIS Terra AOD, and (d) MODIS Aqua AOD for 2005–2015. The small black dot at the each grid box indicates significance at 90% confidence.

and the southern central U.S. (30–40°N, 100–110°W), respectively. Here we use ordinary least squares bisector of the normalized trend of each component to calculate the regression line, which is one of several regression methods applicable for evaluating relationships between two noisy data sets [*Isobe et al.*, 2009]. Since we only compare the grid cells for which the trends have a significance of at least 90% confidence, the blank areas near the axis are due to exclusion of data corresponding to insignificant trends. The trends of AAOD are well correlated with AOD ($r = 0.86$, $N = 504$, $P = 99.9\%$) over the U.S., in particular, over the southern central U.S. ($r = 0.63$, $N = 136$, $P = 99.9\%$). Thus, AAOD enhancements over the south central U.S. may be associated with the same mechanisms driving increases in AOD. Also, there are no points in the quadrant where the AOD trend is positive and the AAOD trend is negative over both the U.S. and the south central U.S., which confirms that the increasing AOD trends are dominated by the increasing AAOD trends. When the AOD trend is <0 and the AAOD trend is >0, there are more retrievals over the whole U.S. and only two grids over the south central U.S., which suggests that a different mechanism may drive increases in AAOD in the south central U.S. than in the rest of the country.

Next we consider the role that trends in precipitation may play in AAOD trends since wet deposition plays an important role in reducing the aerosol concentrations [*Zhang et al.*, 2010]. The monthly precipitation data from NOAA Climate Prediction Center (CPC), which provides a global data set from 1948 to the present [*Chen et al.*, 2008a, 2008b; *Xie et al.*, 2007], are analyzed to calculate trends of wet scavenging. Figures 4c and 4d show the CPC precipitation trends as percentage changes for 2005–2015 in the U.S. and the south central U.S., respectively. As indicated by other studies [*Seager and Hoerling*, 2014; *Wang and Kumar*, 2015; *Rupp et al.*, 2015], a severe drought has been afflicting the southwest U.S. for the past several years. In comparison, the largest enhancements of AAOD and AOD are over the central states of Texas, Oklahoma, Kansas, and Nebraska. Although the trends for AAOD and precipitation are not correlated well over the whole U.S., their correlation coefficient, while still relatively small, shows an enhancement by a factor of 2 ($r = -0.16$, $N = 15$, $P = 40\%$) over the southern central U.S. compared to over the entire U.S. (Figures 4c and 4d).

As pointed out by previous studies, larger AOD is usually associated with suppression of precipitation in the dry season, and the high aerosol concentration is accompanied by negative precipitation anomalies [*Huang*

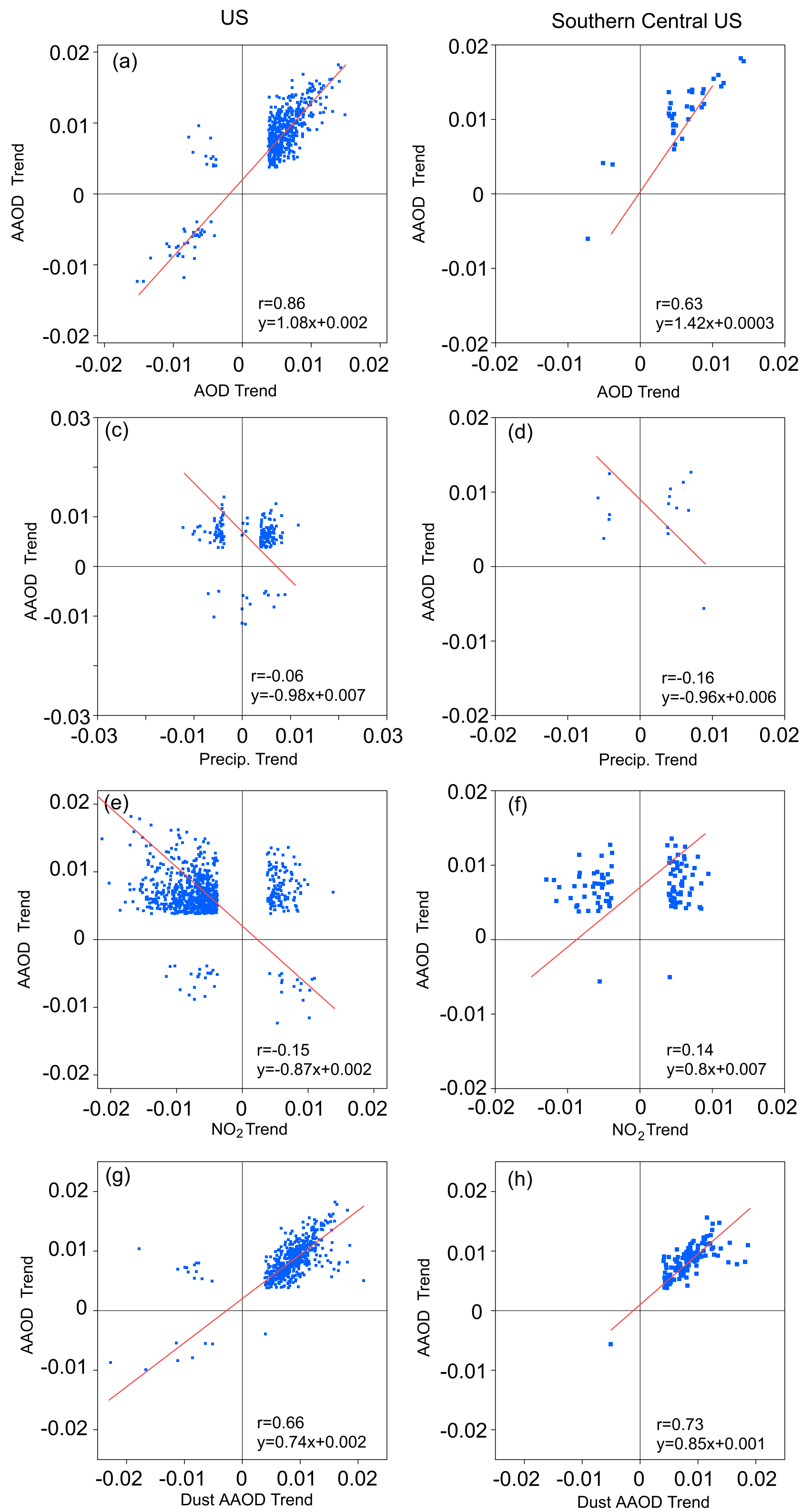

Figure 4. Comparisons of the trends (normalized regression coefficients) for (a and b) AAOD versus AOD, (c and d) AAOD versus precipitation, (e and f) AAOD versus NO_2, and (g and h) AAOD versus dust AAOD for 2005–2015 over the U.S. (20–50°N, 60–130°W) and the southern central U.S. (30–40°N, 100–110°W), respectively.

et al., 2009; *Deng et al.*, 2014]. Decreasing precipitation in these regions may thus partly contribute the enhancements of aerosol concentrations and thus positive trends of both AAOD and AOD.

Due to a combination of environmental policies, technological change, and a reduction of emissions from mobile and point sources [*McDonald et al.*, 2012; *Xing et al.*, 2013], nitrogen dioxide (NO_2) levels have decreased 30–40% in recent decades [*Lamsal et al.*, 2015]. Considering coemissions of BC and NO_x associated with oil and gas activity, we investigate possible correlations between OMI observations of AAOD and NO_2. Figures 4e and 4f show the trends of NO_2 using an improved tropospheric NO_2 VCD data product [*Lamsal et al.*, 2015] correlated with AAOD from OMI for 2005–2015. In contrast to the reduction pattern over most of the U.S., there are also significant positive trends of 50–70% across parts of the central U.S., in particular in states with oil and gas production sources, such as North Dakota and Texas. The trend of AAOD is significantly negatively correlated with NO_2 over the U.S., and positively correlated with NO_2 over the south central U.S., although weakly in both cases (Figures 4e and 4f). Oil and gas production has increased in the last decade over these regions, which may also impact BC emissions (https://www.dmr.nd.gov/oilgas/stats/statisticsvw.asp). The EC emission rate in the Environmental Protection Agency (EPA) National Emissions Inventory Database released in 2013 is 800 t/yr based on 2011, a factor of 2.2 less than observed emissions in 2014 in the Bakken region [*Schwarz et al.*, 2015]. Although the production activities are unlikely to contribute to large-scale biases in estimates of BC emissions on a continental scale, they may possibly impact AAOD not only in the local areas but also in the remote regions. We performed a sensitivity experiment by using GEOS-Chem by increasing anthropogenic BC aerosol emissions by 50% in July of 2012 over the central U.S. led to enhancements of AAOD by 5–10% over the eastern U.S. and southwestern U.S.

Changes in trends of surface concentrations of absorbing aerosols may also provide hints to help explain the observed AAOD trends. The IMPROVE network provides long-term in situ measurements for the surface concentrations for aerosols. Figures 5a–5d illustrate the trends of percentage changes for 151 sites over 43 states based on the measurements of surface EC, OC, dust, and coarse PM from the IMPROVE network. All the black circles indicate the IMPROVE site, and we only show the sites with color where there is significance at the 90% confidence level. Thus, the blank circles indicate site locations where there are not significant trends. Due to the emission control policy for diesel BC emissions, the surface EC concentrations have declined significantly in recent decades over wide areas of the U.S., which has also been discussed in other studies [*McDonald et al.*, 2015; *Murphy et al.*, 2011; *Bahadur et al.*, 2011]. An exception exists in several sites in North Dakota where oil (and gas) production in the Bakken region has increased by a factor of 2.5 (and 2.9) between May 2011 and May 2014, which resulted in enhanced EC emissions [*Schwarz et al.*, 2015]. The OC trends are quite similar to those of EC over the eastern U.S. and southwestern U.S. However, there are fewer sites showing significant decreasing trends, in particular over New Mexico, Colorado, Wyoming, and the northwestern U.S.

Dust aerosols, especially for larger sizes, also exert strong absorption. From the IMPROVE measurements, we find that trends of $PM_{2.5}$ dust concentrations are increasing in some sites over the central U.S. and part of the western U.S. (Figure 5c). The magnitudes of the positive trends are largest over the central U.S. in the states of New Mexico, Texas, Oklahoma, Kansas, and Nebraska. Also, one site in the western U.S. in Oregon and California each have positive trends. Actually, the dust absorption is mainly dominated by the large particles [*Miller et al.*, 2006]. The large aerosols have changed significantly in last decades; the coarse PM from the IMPROVE measurements shows positive trends by 50–100% at the sites over western and central U.S. (Figure 5d), especially, over areas where AAOD has the largest positive trend. Coarse particles primarily originate from geologic sources (soil and other crustal materials), and they typically comprise approximately 50–60% of PM_{10}, although they might make up 90% of PM mass concentrations during dust events [*Ostro et al.*, 1999; *Lin et al.*, 2012].

The OMI OMAERUV retrieval also flags instances for which the retrieval algorithm relies upon the presence of carbonaceous aerosols, dust, and light-absorbing aerosols (mentioned in section 2), that we can use it to quantify the carbonaceous aerosols and dust AAOD. Significant positive trends have only been found in the OMI AAOD flagged for the presence of dust (see Figure 5e) over the western and central U.S., such as eastern California, Nevada, Arizona, Utah, New Mexico, and Colorado. The trends of AAOD are significantly positively correlated with the trends of dust AAOD both over the U.S. ($r = 0.66$, $N = 480$, $P = 99.9\%$) and southern central U.S. ($r = 0.73$, $N = 123$, $P = 99.9\%$, see Figures 4g and 4h).

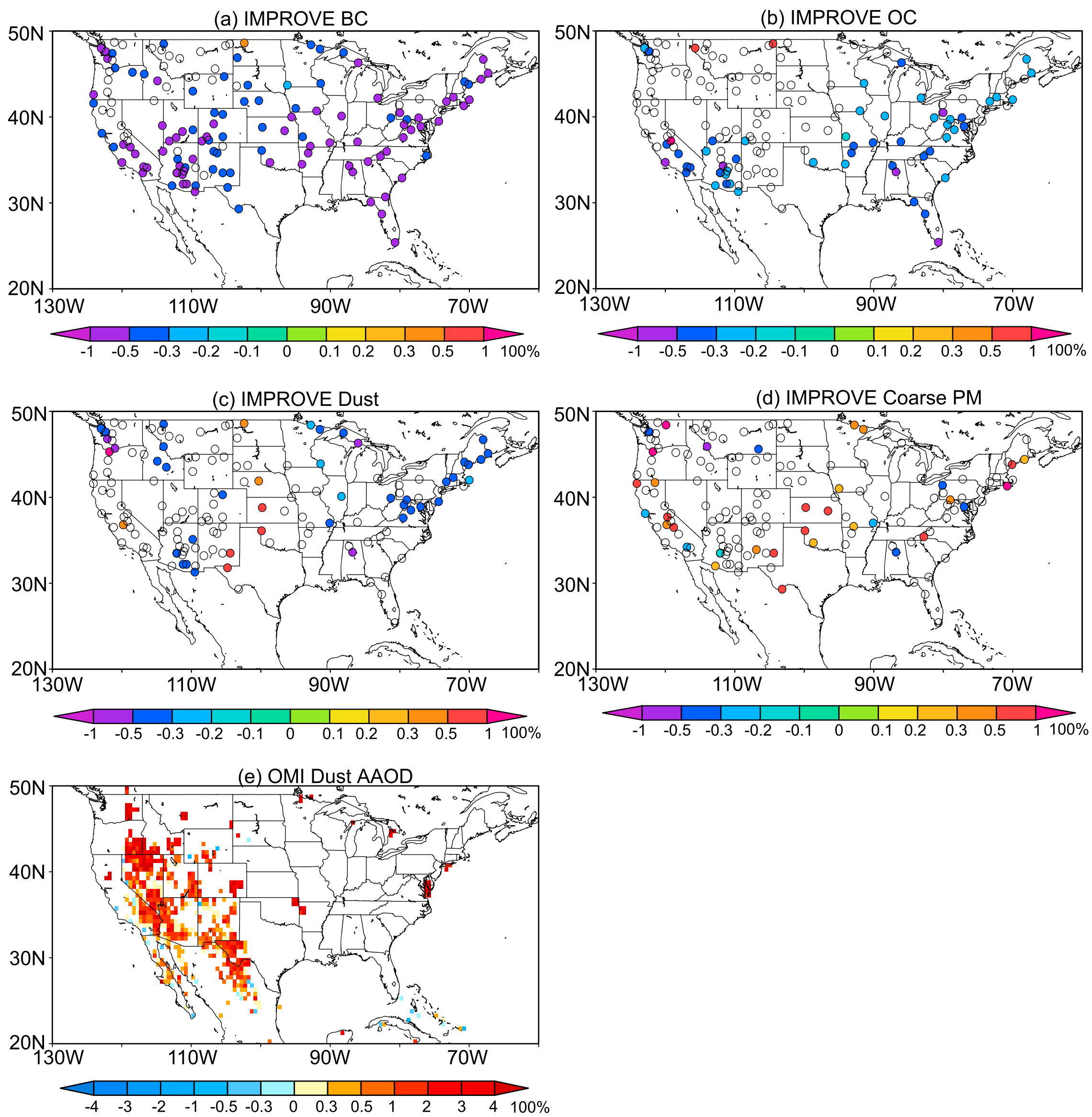

Figure 5. The trends of percentage changes (unit: 100%) for IMPROVE surface concentrations of (a) EC, (b) OC, (c) dust, (d) coarse PM, and (e) OMI dust AAOD for 2005–2015. The circles indicate the IMPROVE sites and only show the sites with color and areas with significance at the 90% confidence level.

This suggests that the changes of dust, either at the surface or throughout the column, are one of the factors contributing to the positive trends of AAOD over the western and central U.S. Compared to the trends of IMPROVE surface dust concentrations, the positive trends of dust AAOD extend over a greater portion of the western U.S. Using satellite-based estimates and model simulations of AOD, *Yu et al.* [2012] pointed out that the imported contribution of dust in the U.S. is dominated (88%) by the trans-Pacific transport from Asia. We performed a sensitivity calculation by using GEOS-Chem, comparing simulations with Asian BC and dust emissions turned off. These indicate that Asian dust and BC contribute about 20–30% and 20–40%, respectively, to the total AAOD over western U.S. in April. Therefore, the positive trends of AAOD over the western U.S. in the spring (MAM) may possibly be due to the trans-Pacific transport from Asia, even though we did not see significant long-range impacts on the U.S. surface dust and BC trends, as trans-Pacific transport has a greater relative impact on concentrations at much higher altitudes above the surface [*Hadley et al.*, 2007]. Another sensitivity calculation was performed in April by doubling the dust emissions in the western U.S. The results of this experiment indicate that this source contributes 5–20% of AAOD in the western U.S.

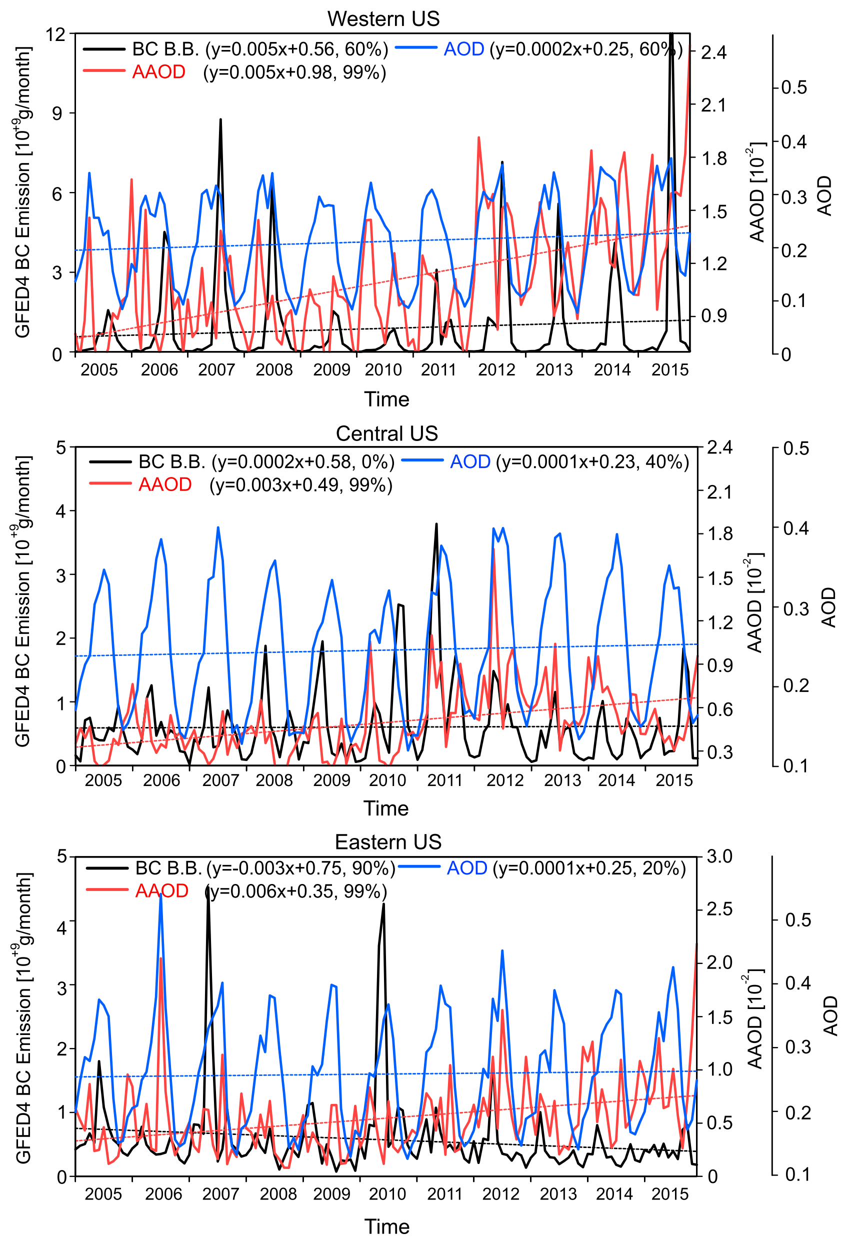

Figure 6. Interannual variability of monthly OMI AAOD, AOD, and GFED4 biomass burning BC emissions over (a) western U.S. (108°–125°W, 30°–50°N), (b) central U.S. (90°–108°W, 25°–50°N), and (c) eastern U.S. (60°–90°W, 25°–50°N).

Another factor that may potentially explain AAOD trends is biomass burning from wildfires. Here we defined three subdomains as the rectangles shown in Figure 1a: western U.S. (108°–125°W, 30°–50°N), central U.S. (90°–108°W, 25°–50°N), and eastern U.S. (60°–90°W, 25°–50°N). The time series of monthly BC biomass burning from the GFED4 inventory [*Giglio et al.*,2013] and AAOD for 2005–2015 are indicated in Figure 6. The solid red and black lines illustrate the trends of these two time series, respectively. Over the western U.S., the interannual variability of BC biomass burning emission reflects the large wildfires in the 2007, 2012, 2013, and 2015. While there were more biomass burning emissions in the last year, the overall trend in the 2005–2015 time period is very small.

The annual variations of AAOD are similar to that of the BC biomass burning; however, the actual timing of the AAOD peaks does not match those of the biomass burning emission of the inventory of either the GFED4 or Fire Inventory from National Center for Atmospheric Research. The variations of AAOD and BC biomass burning over the western U.S. are weakly correlated, and the correlation coefficient is 0.16 ($N = 132$,

$P = 90\%$) and 0.11 ($N = 132$, $P = 60\%$) for the original time series when filtering the seasonal cycle, respectively. Connections between biomass burning and AAOD are even less clear in other regions. Over the central U.S., although AAOD consistently increases in the last several years from 2011, the largest BC biomass burning emissions are from 2010 to 2011 and begin to decrease after 2012. Although their variations are correlated more than those in the western U.S. ($r = 0.21$, $N = 132$, $P = 98\%$), even after filtering out the seasonal cycle ($r = 0.21$, $N = 132$, $P = 98\%$), the biomass burning emission of BC does not contribute to the trend correlation. Similar in the eastern U.S. the interannual variabilities of BC biomass burning and AAOD are not quite consistent—we do not see the enhancements for BC biomass burning from 2012, whereas AAOD increases significantly since 2011. Also, the variation of AAOD does not correlate significantly with that of BC biomass burning ($r = -0.14$, $N = 132$, $P = 80\%$) over the eastern U.S. The impacts of BC biomass burning emissions on the positive trends of AAOD are quite small over central and eastern U.S. From the comparisons of seasonal BC biomass burning emissions and AAOD for 2005–2015 over the above three subdomains (figures not shown), the interannual variability of BC biomass burning emission is consistent with that of AAOD in summer (JJA) and fall (SON) over the western U.S. with the maximum in both 2007, 2012, and 2015. During the summer months (JJA), biomass burning emissions and AAOD are well correlated over the central U.S. We do not see any strong connections between BC biomass burning emissions and AAOD over eastern U.S. for all seasons.

5. Discussion and Conclusions

We examined the spatial and temporal trends of OMI AAOD for the 2005–2015 time frame over the U.S. by using the monthly mean data. The monthly AAOD has increased by a factor of 4 over broad areas, with the maximum enhancements over central U.S. Meanwhile, these positive trends in AAOD consistently occur in all the seasons. Unfortunately, the long-term observations of in situ AAOD are very limited, even for the AERONET network, and none of the sites over the U.S. cover the periods from 2005 to 2015 with continuous AAOD observation, so we were not able to validate these trends in other measurements. However, in this study, in addition to identifying this interesting phenomenon, we also tried to investigate factors that possibly control or contribute to the positive trends of AAOD over the U.S. in last decade. Here we investigated the trends of OMI AOD, precipitation, OMI NO_2, OMI dust AOD, BC biomass burning emission, and IMPROVE in situ measurements of EC, OC, dust, and coarse PM. The positive trend of AAOD is dominated by the trends of dust, as well as a combination of other factors with regional diversity.

First, we did not identify similar positive trends in AOD over broad areas of the U.S., which only show an enhancement over part of the western and southern central U.S. with less spatial coverage than that of AAOD. This suggests that the positive trends of AAOD over broad areas only reflect the enhancement of absorption, not the total aerosol concentrations. NO_2 columns also show positive trends over part of the southern central U.S. in oil and gas production areas (such as Texas and North Dakota), as also recently found in *Duncan et al.* [2016], and are otherwise reduced significantly over most of the eastern and western U.S. Normally, BC is the major absorbing aerosol components and biomass burning emission is one of the important sources of absorbing aerosol concentrations. However, the positive trend of AAOD occurring in all seasons and throughout the entire U.S. is not due to changes of biomass burning. The interannual variability of AAOD is only associated with biomass burning emissions over the western U.S. from 2011 to 2015 in the summer (JJA). Meanwhile, BC (here represented by EC in IMPROVE measurements) and OC surface concentrations show consistently negative trends (except in North Dakota), supported by the decreases in emissions from the U.S. There are more sites indicating positive trends for dust over the central and western U.S. Additionally, trends of OMI dust AAOD are significantly positive, which contribute directly to the enhancements of total AAOD over the south central U.S. and part of the western U.S. The consistent positive trends for both AAOD and AOD over the central U.S. are partly due to the decreasing trends of precipitation that reduce aerosol wet scavenging. However, the data do not suggest that scavenging alone has been reduced significantly enough to explain the observed trends. Precipitation trends may also increase dust emissions associated with dry soil moisture. The multiple regression result shows that AOD and dust AAOD contributions to total AAOD are significant with the same regression coefficient of 0.62 and 0.005, respectively (*$N = 244$, $P = 99.9\%$*) over the U.S.

The transport of absorbing aerosol from upwind source regions may also affect AAOD, including both trans-Pacific transport and domestic transport. There has been a 20–40% increase of anthropogenic BC emissions over Asia in the last decade and more than a 30% increase of exported Asian dust reaching the west coast of North America [*Lu et al*., 2011; *Yu et al*., 2012]. However, it is difficult to quantify the exact contribution of Asian dust and BC to the observed AAOD trends. A series of GEOS-Chem model sensitivity experiments are performed to evaluate the contribution of upwind sources to the AAOD trends. These experiments show that if BC and dust emissions were doubled over Asia and over the western and central U.S., respectively, it would result in increasing the AAOD by 40–70% and 35–60% over the western and central U.S. in April. Since emissions have not increased by that amount in either source region, and yet there is a 50–100% positive trend of OMI AAOD in the U.S., the latter must be a combined effect from both long-range transport and domestic impacts.

Another possible factor is the contribution of brown carbon, which has an aerosol radiative forcing greater than 20–50% over regions dominated by seasonal biomass burnings and biofuel combustion, accounting for more than 25% of the estimated radiative effects of BC on a global scale [*Feng et al*., 2013]. Assuming that the AAOD impact on radiative effects is linear for both brown carbon and BC, an enhancement of brown carbon by 200% in the last decade would be required to explain the observed 50% increase of AAOD over the west central U.S., which seems unlikely. Meanwhile, changes of dust emissions and concentrations can be driven by several aspects of climate. Trends of dust AAOD depend not only upon changes of total dust emissions but also associated changes of size distributions. A subset of wind tunnel studies found that dust aerosol size decreases with increasing wind speed [*Rea*, 1994; *Ding et al*., 2002; *Ruth et al*., 2003]. However, other wind tunnel measurements and field studies have not found a clear dependence of the emitted dust size distribution on wind speed [*Shao et al*., 2011; *Kok*, 2011a]. Meanwhile, a recently formulated brittle fragmentation theory predicts that the emitted dust size distribution is independent of wind speed [*Kok*, 2011a, 2011b; *Zhang et al*., 2013]. Fugitive dust, PM suspended in the air by wind action and human activates, or dust not coming from a combustion source, accounts for about 90% of all primary PM_{10} emissions over California recently (https://www.arb.ca.gov/pm/fugitivedust_large.pdf). Changes in concentrations of larger fugitive dust would enhance the AAOD. The above studies do, however, consistently suggest that changes to soil texture associated with climate change do impact emitted dust size distributions. Other possible confounding factors could include changes to optical properties of absorbing aerosols associated with internal mixing, their lifetime due to climate changes, and large-scale interannual meteorological variability [*Zhang and Iwasaka*, 2004; *Zhang and Iwasaka*, 2006; *Zhang et al*., 2010; *Zhu et al*., 2012]. Lastly, when using a retrieval algorithm that includes a threshold for small values of AOD, such as OMAERUV version 1.4.2., analysis of AAOD trends may be different than those without using a threshold, as the threshold would weight the trend toward changes in polluted areas, excluding the background impacts more closely associated with dust event, biomass burning activities, or aerosol composition changes.

Acknowledgments
This work was supported from NASA grant NNX15AC30G and the Environmental Protection Agency (EPA) -STAR grant RD-83503701-0. Although the research described in the article has been funded wholly or in part by the U. S. EPA's STAR program through grant (RD-83503701-0), it has not been subjected to any EPA review and therefore does not necessarily reflect the views of the Agency, and no official endorsement should be inferred. The OMI data for this paper are freely available from https://earthdata.nasa.gov/ and properly cited and referred to in the reference list. The Interagency Monitoring of Protected Visual Environment (IMPROVE) data are freely available at http://vista.cira.colostate.edu/improve/. The source code for the GEOS-Chem model used in this study is freely available at http://acmg.seas.harvard.edu/geos/. The authors would like to thank the anonymous reviewers for their insightful comments and suggestions that have contributed to improve this paper.

References

Ahn, C., O. Torres, and H. Jethva (2014), Assessment of OMI near-UV aerosol optical depth over land, *J. Geophys. Res. Atmos.*, *119*, 2457–2473, doi:10.1002/2013JD020188.

Alpert, P., O. Shvainshtein, and P. Kishcha (2012), AOD trends over megacities based on space monitoring using MODIS and MISR, *Am. J. Clim. Change*, *1*(3), 117–131, doi:10.4236/ajcc.2012.13010.

Bahadur, R., Y. Feng, L. M. Russell, and V. Ramanathan (2011), Impact of California's air pollution laws on black carbon and their implications for direct radiative forcing, *Atmos. Environ.*, *45*, 1162–1167.

Bergstrom, R. W., P. Pilewskie, P. B. Russell, J. Redemann, T. C. Bond, P. K. Quinn, and B. Sierau (2007), Spectral absorption properties of atmospheric aerosols, *Atmos. Chem. Phys.*, *7*, 5937–5943, doi:10.5194/acp-7-5937-2007.

Bey, I., D. J. Jacob, R. M. Yantosca, J. A. Logan, B. D. Field, A. M. Fiore, Q. Li, H. Y. Liu, L. J. Mickley, and M. G. Schultz (2001), Global modeling of tropospheric chemistry with assimilated meteorology: Model description and evaluation, *J. Geophys. Res.*, *106*(D19), 23,073–23,095, doi:10.1029/2001JD000807.

Bond, T. C., D. G. Streets, K. F. Yarber, S. M. Nelson, J.-H. Woo, and Z. Klimont (2004), A technology-based global inventory of black and organic carbon emissions from combustion, *J. Geophys. Res.*, *109*, D14203, doi:10.1029/2003JD003697.

Bond, T. C., E. Bhardwaj, R. Dong, R. Jogani, S. Jung, C. Roden, D. G. Streets, and N. M. Trautmann (2007), Historical emissions of black and organic carbon aerosol from energy-related combustion, 1850–2000, *Global Biogeochem. Cycles*, *21*, GB2018, doi:10.1029/2006GB002840.

Chen, M., W. Shi, P. Xie, V. B. S. Silva, V. E. Kousky, R. Wayne Higgins, and J. E. Janowiak (2008a), Assessing objective techniques for gauge-based analyses of global daily precipitation, *J. Geophys. Res.*, *113*, D04110, doi:10.1029/2007JD009132.

Chen, M., et al. (2008b), CPC unified gauge-based analysis of global daily precipitation, Western Pacific geophysics meeting, Cairns, Australia, 29 July–1 August.

Chin, M., P. Ginoux, S. Kinne, O. Torres, B. N. Holben, B. N. Duncan, R. V. Martin, J. A. Logan, A. Higurashi, and T. Nakajima (2002), Tropospheric aerosol optical thickness from the GOCART model and comparisons with satellite and Sun photometer measurements, *J. Atmos. Sci.*, *59*, 461–483.

Cooke, W. F., C. Liousse, H. Cachier, and J. Feichter (1999), Construction of a 1° × 1° fossil fuel emission data set for carbonaceous aerosol and implementation and radiative impact in the ECHAM4 model, *J. Geophys. Res.*, *104*(D18), 22,137–22,162, doi:10.1029/1999JD900187.

Dawson, J. P., P. J. Adams, and S. N. Pandis (2007), Sensitivity of PM2.5 to climate in the Eastern US: A modeling case study, *Atmos. Chem. Phys.*, *7*, 4295–4309, doi:10.5194/acp-7-4295-2007.

Deng, Y., T. Gao, H. Gao, X. Yao, and L. Xie (2014), Regional precipitation variability in East Asia related to climate and environmental factors during 1979–2012, *Sci. Rep.*, *4*, 5693, doi:10.1038/srep05693.

Ding, Z. L., E. Derbyshire, S. L. Yang, Z. W. Yu, S. F. Xiong, and T. S. Liu (2002), Stacked 2.6-Ma grain size record from the Chinese loess based on five sections and correlation with the deep-sea _18O record, *Paleoceanography*, *17*(3), 1033, doi:10.1029/2001PA000725.

Duncan, B. N., L. N. Lamsal, A. M. Thompson, Y. Yoshida, Z. Lu, D. G. Streets, M. M. Hurwitz, and K. E. Pickering (2016), A space-based, high-resolution view of notable changes in urban NOx pollution around the world (2005–2014), *J. Geophys. Res. Atmos.*, *121*(2), 976–996, doi:10.1002/2015JD024121.

Eguchi, K., I. Uno, K. Yumimoto, T. Takemura, A. Shimizu, N. Sugimoto, and Z. Liu (2009), Trans-Pacific dust transport: Integrated analysis of NASA/CALIPSO and a global aerosol transport model, *Atmos. Chem. Phys.*, *9*, 3137–3145, doi:10.5194/acp-9-3137-2009.

Fairlie, T. D., D. J. Jacob, and R. J. Park (2007), The impact of transpacific transport of mineral dust in the United States, *Atmos. Environ.*, *41*, 1251–1266, doi:10.1016/j.atmosenv.2006.09.048.

Feng, Y., V. Ramanathan, and V. R. Kotamarthi (2013), Brown carbon: A significant atmospheric absorber of solar radiation?, *Atmos. Chem. Phys.*, *13*, 8607–8621, doi:10.5194/acp-13-8607-2013.

Giglio, L., J. T. Randerson, and G. R. van der Werf (2013), Analysis of daily, monthly, and annual burned area using the fourth-generation Global Fire Emissions Database (GFED4), *J. Geophys. Res. Biogeosci.*, *118*, 317–328, doi:10.1002/jgrg.20042.

Ginoux, P., M. Chin, I. Tegen, J. M. Prospero, B. Holben, O. Dubovik, and S.-J. Lin (2001), Sources and distributions of dust aerosols simulated with the GOCART model, *J. Geophys. Res.*, *106*(D17), 20,255–20,273, doi:10.1029/2000JD000053.

Ginoux, P., J. M. Prospero, O. Torres, and M. Chin (2004), Long-term simulation of global dust distribution with the GOCART model: Correlation with North Atlantic oscillation, *Environ. Modell. Software*, *19*, 113–128.

Hadley, O. L., V. Ramanathan, G. R. Carmichael, Y. Tang, C. E. Corrigan, G. C. Roberts, and G. S. Mauger (2007), Trans-Pacific transport of black carbon and fine aerosols ($D < 2.5\ \mu m$) into North America, *J. Geophys. Res.*, *112*, D05309, doi:10.1029/2006JD007632.

Huang, J., P. Minnis, B. Chen, Z. Huang, Z. Liu, Q. Zhao, Y. Yi, and J. K. Ayers (2008), Long-range transport and vertical structure of Asian dust from CALIPSO and surface measurements during PACDEX, *J. Geophys. Res.*, *113*, D23212, doi:10.1029/2008JD010620.

Huang, J., C. Zhang, and J. M. Prospero (2009), African aerosol and large-scale precipitation variability over West Africa, *Environ. Res. Lett.*, *4*, 015006, doi:10.1088/1748-9326/4/1/015006.

Isobe, T., E. D. Feigelson, M. G. Akritas, and G. J. Babu (2009), Linear regression in astronomy, *Astrophys. J.*, *364*, 104–113.

Jethva, H., O. Torres, and C. Ahn (2014), Global assessment of OMI aerosol single-scattering albedo using ground-based AERONET inversion, *J. Geophys. Res. Atmos.*, *119*, 9020–9040, doi:10.1002/2014JD021672.

Kok, J. F. (2011a), Does the size distribution of mineral dust aerosols depend on the wind speed at emission?, *Atmos. Chem. Phys.*, *11*, 10,149–10,156, doi:10.5194/acp-11-10149-2011.

Kok, J. F. (2011b), A scaling theory for the size distribution of emitted dust aerosols suggests climate models underestimate the size of the global dust cycle, *Proc. Natl. Acad. Sci. U.S.A.*, *108*(3), 1016–1021.

Lack, D. A., and C. D. Cappa (2010), Impact of brown and clear carbon on light absorption enhancement, single scatter albedo and absorption wavelength dependence of black carbon, *Atmos. Chem. Phys.*, *10*, 4207–4220, doi:10.5194/acp-10-4207-2010.

Lamsal, L., B. Duncan, Y. Yoshida, N. Krotkov, K. Pickering, D. Streets, and Z. Lu (2015), U.S. NO_2 trends (2005–2013): EPA Air Quality System (AQS) data versus improved observations from the Ozone Monitoring Instrument (OMI), *Atmos. Environ.*, *110*, 130–143.

Levelt, P. F., G. H. J. van den Oord, M. R. Dobber, A. Mälkki, H. Visser, J. de Vries, P. Stammes, J. O. V. Lundell, and H. Saari (2006), The Ozone Monitoring Instrument, *IEEE Trans. Geosci. Remote Sens.*, *44*(5), 1093–1101, doi:10.1109/TGRS.2006.872333.

Lewis, K., W. P. Arnott, H. Moosmüller, and C. E. Wold (2008), Strong spectral variation of biomass smoke light absorption and single scattering albedo observed with a novel dual-wavelength photoacoustic instrument, *J. Geophys. Res.*, *113*, D16203, doi:10.1029/2007JD009699.

Lin, C.-Y., Y.-F. Sheng, W.-N. Chen, Z. Wang, C.-H. Kuo, W.-C. Chen, and T. Yang (2012), The impact of channel effect on Asian dust transport dynamics: A case in southeastern Asia, *Atmos. Chem. Phys.*, *12*, 271–285, doi:10.5194/acp-12-271-2012.

Liu, H., D. J. Jacob, I. Bey, and R. M. Yantosca (2001), Constraints from 210Pb and 7Be on wet deposition and transport in a global three-dimensional chemical tracer model driven by assimilated meteorological fields, *J. Geophys. Res.*, *106*(D11), 12,109–12,128, doi:10.1029/2000JD900839.

Logan, T., B. Xi, X. Dong, Z. Li, and M. Cribb (2013), Classification and investigation of Asian aerosol absorptive properties, *Atmos. Chem. Phys.*, *13*, 2253–2265, doi:10.5194/acp-13-2253-2013.

Lu, Z., Q. Zhang, and D. G. Streets (2011), Sulfur dioxide and primary carbonaceous aerosol emissions in China and India, 1996–2010, *Atmos. Chem. Phys.*, *11*, 9839–9864, doi:10.5194/acp-11-9839-2011.

Ma, X., F. Yu, and G. Luo (2012), Aerosol direct radiative forcing based on GEOS-Chem-APM and uncertainties, *Atmos. Chem. Phys.*, *12*, 5563–5581, doi:10.5194/acp-12-5563-2012.

Malm, W. C., J. F. Sisler, D. Huffman, R. A. Eldred, and T. A. Cahill (1994), Spatial and seasonal trends in particle concentration and optical extinction in the United States, *J. Geophys. Res.*, *99*(D1), 1347–1370, doi:10.1029/93JD02916.

Martin, R. V., D. J. Jacob, R. M. Yantosca, M. Chin, and P. Ginoux (2003), Global and regional decreases in tropospheric oxidants from photochemical effects of aerosols, *J. Geophys. Res.*, *108*(D3), *4097*, doi:10.1029/2002JD002622.

McDonald, B. C., T. R. Dallmann, E. W. Martin, and R. A. Harley (2012), Long-term trends in nitrogen oxide emissions from motor vehicles at national, state, and air basin scales, *J. Geophys. Res.*, *117*, D00V18, doi:10.1029/2012JD018304.

McDonald, C. B., A. H. Goldstein, and R. A. Harley (2015), Long-term trends in California mobile source emissions and ambient concentrations of black carbon and organic aerosol, *Environ. Sci. Technol.*, *49*(8), 5178–5188, doi:10.1021/es505912b.

Miller, R. L., et al. (2006), Mineral dust aerosols in the NASA Goddard Institute for Space Sciences ModelE atmospheric general circulation model, *J. Geophys. Res.*, *111*, D06208, doi:10.1029/2005JD005796.

Mu, Q., and H. Liao (2014), Simulation of the interannual variations of aerosols in China: Role of variations in meteorological parameters, *Atmos. Chem. Phys.*, *14*, 9597–9612, doi:10.5194/acp-14-9597-2014.

Murphy, D. M., J. C. Chow, E. M. Leibensperger, W. C. Malm, M. Pitchford, B. A. Schichtel, J. G. Watson, and W. H. White (2011), Decreases in elemental carbon and fine particle mass in the United States, *Atmos. Chem. Phys.*, *11*, 4679–4686, doi:10.5194/acp-11-4679-2011.

Myhre, G. (2009), Consistency between satellite-derived and modeled estimates of the direct aerosol effect, *Science*, *325*(5937), 187–190.

Myhre, G., et al. (2013), Anthropogenic and natural radiative forcing, in *Climate Change 2013: The Physical Science Basis. Working Group I Contribution to the IPCC Fifth Assessment Report*, edited by T. F. Stocker et al., pp. 661–740, Cambridge Univ. Press, Cambridge, U. K. [Available at http://www.ipcc.ch/report/ar5/wg1/.]

Ostro, B. D., S. Hurley, and M. J. Lipsett (1999), Air pollution and daily mortality in the Coachella Valley, California: A study of PM10 dominated by coarse particles, *Environ. Res.*, *81*, 231–238.

Park, R. J., D. J. Jacob, M. Chin, and R. V. Martin (2003), Sources of carbonaceous aerosols over the United States and implications for natural visibility, *J. Geophys. Res.*, *108*(D12), *4355*, doi:10.1029/2002JD003190.

Rea, D. K. (1994), The paleoclimatic record provided by eolian deposition in the deep sea: The geologic history of wind, *Rev. Geophys.*, *32*(2), 159–195, doi:10.1029/93RG03257.

Ridley, D. A., C. L. Heald, and J. M. Prospero (2014), What controls the recent changes in African mineral dust aerosol across the Atlantic?, *Atmos. Chem. Phys.*, *14*, 5735–5747, doi:10.5194/acp-14-5735-2014.

Rupp, D. E., S. Li, N. Massey, S. N. Sparrow, P. W. Mote, and M. Allen (2015), Anthropogenic influence on the changing likelihood of an exceptionally warm summer in Texas, 2011, *Geophys. Res. Lett.*, *42*, 2392–2400, doi:10.1002/2014GL062683.

Russell, P. B., R. W. Bergstrom, Y. Shinozuka, A. D. Clarke, P. F. DeCarlo, J. L. Jimenez, J. M. Livingston, J. Redemann, O. Dubovik, and A. Strawa (2010), Absorption Angstrom exponent in AERONET and related data as an indicator of aerosol composition, *Atmos. Chem. Phys.*, *10*, 1155–1169, doi:10.5194/acp-10-1155-2010.

Ruth, U., D. Wagenbach, J. P. Steffensen, and M. Bigler (2003), Continuous record of microparticle concentration and size distribution in the central Greenland NGRIP ice core during the last glacial period, *J. Geophys. Res.*, *108*(D3), *4098*, doi:10.1029/2002JD002376.

Schwarz, J. P., J. S. Holloway, J. M. Katich, S. McKeen, E. A. Kort, M. L. Smith, T. B. Ryerson, C. Sweeney, and J. Peischl (2015), Black carbon emissions from the Bakken oil and gas development region, *Environ. Sci. Tech. Lett.*, *2*(10), 281–285, doi:10.1021/acs.estlett.5b00225.

Seager, R., and M. Hoerling (2014), Atmosphere and ocean origins of North American droughts, *J. Clim.*, *27*, 4581–4606, doi:10.1175/JCLI-D-13-00329.1.

Shao, Y., M. Ishizuka, M. Mikami, and J. F. Leys (2011), Parameterization of size-resolved dust emission and validation with measurements, *J. Geophys. Res.*, *116*, D08203, doi:10.1029/2010JD014527.

Shao, Y., M. Klose, and K.-H. Wyrwoll (2013), Recent global dust trend and connections to climate forcing, *J. Geophys. Res. Atmos.*, *118*, 11,107–11,118, doi:10.1002/jgrd.50836.

Sneyers, R. (1990), On the statistical analysis of series of observations, *WMO Tech. Note 143*.

Torres, O., A. Tanskanen, B. Veihelmann, C. Ahn, R. Braak, P. K. Bhartia, P. Veefkind, and P. Levelt (2007), Aerosols and surface UV products from Ozone Monitoring Instrument observations: An overview, *J. Geophys. Res.*, *112*, D24S47, doi:10.1029/2007JD008809.

Torres, O., C. Ahn, and Z. Chen (2013), Improvements to the OMI near-UV aerosol algorithm using A-train CALIOP and AIRS observations, *Atmos. Meas. Tech.*, *6*, 3257–3270, doi:10.5194/amt-6-3257-2013.

Wang, H., and A. Kumar (2015), Assessing the impact of ENSO on drought in the U.S. Southwest with NCEP climate model simulations, *J. Hydrol.*, *526*, 30–41.

Wang, Y., D. J. Jacob, and J. A. Logan (1998), Global simulation of tropospheric O3-NO*x*-hydrocarbon chemistry: 3. Origin of tropospheric ozone and effects of nonmethane hydrocarbons, *J. Geophys. Res.*, *103*(D9), 10,757–10,767, doi:10.1029/98JD00156.

Wesely, M. L. (1989), Parameterization of surface resistance to gaseous dry deposition in regional-scale numerical models, *Atmos. Environ.*, *23*, 1293–1304.

Xie, P., A. Yatagai, M. Chen, T. Hayasaka, Y. Fukushima, C. Liu, and S. Yang (2007), A gauge-based analysis of daily precipitation over East Asia, *J. Hydrometeorol.*, *8*, 607–626.

Xing, J., J. Pleim, R. Mathur, G. Pouliot, C. Hogrefe, C.-M. Gan, and C. Wei (2013), Historical gaseous and primary aerosol emissions in the United States from 1990 to 2010, *Atmos. Chem. Phys.*, *13*, 7531–7549, doi:10.5194/acp-13-7531-2013.

Yu, H. B., L. A. Remer, M. Chin, H. S. Bian, Q. Tan, T. L. Yuan, and Y. Zhang (2012), Aerosols from overseas rival domestic emissions over North America, *Science*, *337*, 566–569.

Zender, C. S., H. Bian, and D. Newman (2003), Mineral Dust Entrainment and Deposition (DEAD) model: Description and 1990s dust climatology, *J. Geophys. Res.*, *108*(D14), 4416, doi:10.1029/2002JD002775.

Zhang, D. Z., and Y. Iwasaka (2004), Size change of Asian dust particles caused by sea salt interaction: Measurements in southwestern Japan, *Geophys. Res. Lett.*, *31*, L15102, doi:10.1029/2004GL020087.

Zhang, D. Z., and Y. Iwasaka (2006), Comparison of size changes of Asian dust particles caused by sea salt and sulfate, *J. Meteorol. Soc. Japan.*, *84*(5), 939–947.

Zhang, L., H. Liao, and J. Li (2010), Impacts of Asian summer monsoon on seasonal and interannual variations of aerosols over eastern China, *J. Geophys. Res.*, *115*, D00K05, doi:10.1029/2009JD012299.

Zhang, L., J. F. Kok, D. K. Henze, Q. Li, and C. Zhao (2013), Improving simulations of fine dust surface concentrations over the western United States by optimizing the particle size distribution, *Geophys. Res. Lett.*, *40*, 3270–3275, doi:10.1002/grl.50591.

Zhang, L., et al. (2015), Constraining black carbon aerosol over Asia using OMI aerosol absorption optical depth and the adjoint of GEOS-Chem, *Atmos. Chem. Phys.*, *15*, 10,281–10,308, doi:10.5194/acp-15-10281-2015.

Zhao, C., X. Liu, L. R. Leung, B. Johnson, S. A. McFarlane, W. I. Gustafson Jr., J. D. Fast, and R. Easter (2010), The spatial distribution of mineral dust and its shortwave radiative forcing over North Africa: Modeling sensitivities to dust emissions and aerosol size treatments, *Atmos. Chem. Phys.*, *10*, 8821–8838, doi:10.5194/acp-10-8821-2010.

Zhu, J., H. Liao, and J. Li (2012), Increases in aerosol concentrations over eastern China due to the decadal-scale weakening of the East Asian summer monsoon, *Geophys. Res. Lett.*, *39*, L09809, doi:10.1029/2012GL051428.